

FORMATION OF THE LATERAL SHEAR INTERFEROGRAMS IN DIFFUSELY SCATTERED FIELDS IN THE CASE OF TWO-EXPOSURE RECORDING OF A LENS GABOR HOLOGRAM

V.G. Gusev

*Tomsk State University,
Received May 25, 1995*

The lateral shear interferometer is analyzed using two-exposure recording of lens Gabor hologram of the imaginary image of an amplitude light scatterer. It is shown, that the interference pattern formed in the course of spatial filtering of a diffraction field determines the axial aberration of a lens with double sensitivity.

As it was shown in Ref. 1, at the stage of reconstructing the hologram of an imaginary image of a mat screen illuminated with an aberration-free diverging wave, two-exposure off-axis recording of the hologram using positive lens leads to formation in (-1) diffraction order of lateral shear interferograms in the bands of infinite width. Therewith, the interference pattern, which characterizes wave aberrations of a lens, localizes in the image plane of a mat screen and spatial filtering of the diffraction field in the hologram plane is required to record that pattern. In addition to the object channel, phase distortion in the off-axis reference wave channel appearing due to optical aberrations and forming quasi-plane wave front occurs, as well. The interference pattern, characterizing these distortions, localizes in the hologram plane. The pattern can be recorded in the course of spatial filtering of the diffraction field on the optical axis in the image plane of a mat screen.

In this paper, we analyze peculiarities of the lateral shear interferogram formation in diffusely scattered fields at two-exposure recording of a hologram using Gabor scheme in comparison with the case when the off-axis reference wave is used.

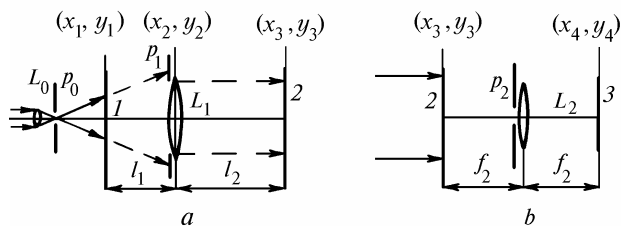


FIG. 1. Optical arrangement of recording (a) and reconstructing (b) of double-exposure Gabor hologram: 1, 2, 3 are amplitude light scatterer, photoplate-hologram, and the plane of the hologram recording, respectively, L_0, L_1, L_2 are lenses, p_0, p_2 are filtering apertures, p_1 is the objective aperture.

As is seen from Fig. 1a, the amplitude light screen located in the plane (x_1, y_1) is illuminated with a coherent aberration-free radiation of diverging spherical wave with the radius of curvature R formed

by lens L_0 and point aperture in an opaque screen p_0 , located at the lens focus. Then, diffusely scattered radiation passes through a controllable lens L_1 with the focal length f_1 and the hologram recording is made on a photoplate 2 during the first exposure. Before the second exposure, the screen is moved in its plane, for example, along the axes x at a distance a , while the photoplate is moved in the same direction at a distance $b = af_1/(f_1 - l_1)$, where l_1 is a distance between the screen and the principal plane (x_2, y_2) of the lens L_1 .

If condition $f_1 > l_1 l_2 / (l_1 + l_2)$ (where l_2 is a distance between the principal plane and the photoplate) holds, in the Fresnel approximation without considering constant factors and based on Ref. 1 complex amplitudes of the fields of the first and second exposures in the plane (x_3, y_3) of the photoplate take the following form:

$$\begin{aligned}
 u_1(x_3, y_3) &\sim \exp \left[\frac{ik (l_2 - L)}{2l_2^2} (x_3^2 + y_3^2) \right] \times \\
 &\times \left\{ [\delta(x_3, y_3) - F(x_3, y_3)] \otimes \right. \\
 &\otimes \exp \left[-\frac{ik (f_1 - l_1) L}{2f_1 l_1 l_2} (x_3^2 + y_3^2) \right] \otimes P_1(x_3, y_3) \left. \right\}, \quad (1) \\
 u_2(x_3, y_3) &\sim \exp \left[\frac{ik (l_2 - L)}{2l_2^2} (x_3^2 + y_3^2) \right] \times \\
 &\times \left\{ [\delta(x_3, y_3) - F(x_3, y_3)] \otimes \right. \\
 &\otimes \exp \left[-\frac{ik (f_1 - l_1) L}{2f_1 l_1 l_2} (x_3^2 + y_3^2) \right] \otimes \\
 &\otimes \exp \left(-i k a x_3 \frac{L}{l_1 l_2} \right) P_1(x_3, y_3) \left. \right\}, \quad (2)
 \end{aligned}$$

where \otimes designates convolution, k is the wave number, $\delta(x_3, y_3)$ is Dirac delta-function,

$$1/L = 1/l_1 - 1/f_1 + 1/l_2,$$

$$F(x_3, y_3) =$$

$$= \int_{-\infty}^{\infty} \int_{-\infty}^{\infty} t(x_1, y_1) \exp[-ik(x_1 x_3 + y_1 y_3) L/l_1 l_2] dx_1 dy_1$$

is the Fourier transform of a diffuse screen which absorption amplitude $t(x_1, y_1)$ is a random function of position,

$$P_1(x_3, y_3) = \int_{-\infty}^{\infty} \int_{-\infty}^{\infty} p_1(x_2, y_2) \exp i \varphi(x_2, y_2) \times$$

$$\times \exp[-ik(x_2 x_3 + y_2 y_3) / l_2] dx_2 dy_2$$

is the Fourier transform of a generalized function $p_1(x_2, y_2) \exp i \varphi(x_2, y_2)$ of the controllable lens pupil (see Ref. 2), with the account for its axial wave aberrations.

If a photolayer exposed with a light of intensity $I(x_3, y_3) = u_1(x_3, y_3) u_1^*(x_3, y_3) + u_2(x_3, y_3) u_2^*(x_3, y_3)$, is developed so that the negative is made within linear segment of the characteristic curve of its blackening and diffusely scattered component of the hologram transmittance, presented in Fig. 1, *b*, with the account for condition $t(x_1, y_1) \ll 1$ is defined by the following expression:

$$\begin{aligned} \tau(x_3, y_3) \sim & [\exp(-i\alpha) \otimes P_1(x_3, y_3)] [F^*(x_3, y_3) \otimes \\ & \otimes \exp(i\alpha) \otimes P_1^*(x_3, y_3)] + [\exp(i\alpha) \otimes P_1^*(x_3, y_3)] \times \\ & \times [F(x_3, y_3) \otimes \exp(-i\alpha) \otimes P_1(x_3, y_3)] + \\ & + [\exp(-i\alpha) \otimes \exp(-ikax_3 L / l_1 l_2) P_1(x_3, y_3)] \times \\ & \times [F^*(x_3, y_3) \otimes \exp(i\alpha) \otimes \exp(ikax_3 L / l_1 l_2) P_1^*(x_3, y_3)] + \\ & + [\exp(i\alpha) \otimes \exp(ikax_3 L / l_1 l_2) \times P_1^*(x_3, y_3)] \times \\ & \times [F(x_3, y_3) \otimes \exp(-i\alpha) \otimes \exp(-ikax_3 L / l_1 l_2) P_1(x_3, y_3)], \end{aligned} \quad (3)$$

where designation $\alpha = \frac{k(f_1 - l_1)L}{2f_1 l_1 l_2} (x_3^2 + y_3^2)$ is used to reduce size of expressions.

Let us assume that spatial filtering of the diffraction field is made at the optical axis of the lens L_2 with the focal length f_2 using the objective pupil aperture p_2 (see Fig. 1, *b*). In this case, according to Ref. 3, distribution of the field complex amplitude in the second focal plane of the lens can be written in the following form:

$$u(x_4, y_4) \sim \int_{-\infty}^{\infty} \int_{-\infty}^{\infty} \tau(x_3, y_3) \exp[-ik(x_3 x_4 + y_3 y_4) / f_2] dx_3 dy_3 \otimes$$

$$\otimes P_2(x_4, y_4), \quad (4)$$

where $P_2(x_4, y_4)$ is the Fourier transform of the transmission function of the objective aperture.

Substitution of Eq. (3) into Eq. (4) gives

$$\begin{aligned} u(x_4, y_4) \sim & [\exp(i\beta) p_1(-\mu_2 x_4, -\mu_2 y_4) \times \\ & \times \exp i \varphi(-\mu_2 x_4, -\mu_2 y_4) \otimes t(\mu_1 x_4, \mu_1 y_4) \exp(-i\beta) \times \\ & \times p_1(\mu_2 x_4, \mu_2 y_4) \exp -i \varphi(\mu_2 x_4, \mu_2 y_4) + \exp(-i\beta) \times \\ & \times p_1(\mu_2 x_4, \mu_2 y_4) \exp -i \varphi(\mu_2 x_4, \mu_2 y_4) \otimes t(-\mu_1 x_4, -\mu_1 y_4) \times \\ & \times \exp(i\beta) p_1(-\mu_2 x_4, -\mu_2 y_4) \exp i \varphi(-\mu_2 x_4, -\mu_2 y_4) + \\ & + \exp(i\beta) p_1(-\mu_2 x_4 - c, -\mu_2 y_4) \exp i \varphi(-\mu_2 x_4 - c, -\mu_2 y_4) \otimes \\ & \otimes t(\mu_1 x_4, \mu_1 y_4) \exp(-i\beta) p_1(\mu_2 x_4 - c, \mu_2 y_4) \times \\ & \times \exp -i \varphi(\mu_2 x_4 - c, \mu_2 y_4) + \exp(-i\beta) \times \\ & \times p_1(\mu_2 x_4 - c, \mu_2 y_4) \exp -i \varphi(\mu_2 x_4 - c, \mu_2 y_4) \otimes \\ & \otimes t(-\mu_1 x_4, -\mu_1 y_4) \exp(i\beta) p_1(-\mu_2 x_4 - c, -\mu_2 y_4) \times \\ & \times \exp i \varphi(-\mu_2 x_4 - c, -\mu_2 y_4)] \otimes P_2(x_4, y_4), \end{aligned} \quad (5)$$

where $\mu_1 = l_1 l_2 / L f_2$, $\mu_2 = l_2 / f_2$ are the coefficients of the scale transformation,

$$\beta = k(x_4^2 + y_4^2) f_1 l_1 l_2 / 2(f_1 - l_1) L f_2^2, \text{ and } c = aL / l_1.$$

Equation (5) describes complex amplitude of the light which produces in the Fourier plane illuminance characteristic of the subjective speckle-structure. The size of individual speckle in this plane is defined by the width of the function $P_2(x_4, y_4)$. Therewith, as can be seen from Eq. 5, if the diameter of illuminated area of the amplitude light reflecting screen is no less than $d_1 \left(1 + \frac{l_1}{l_2} - \frac{l_1}{f_1}\right)$ where d_1 is the pupil diameter of the lens L_1 (see Fig. 1, *a*), the light field in the observation plane for both (-1) and (+1) orders of diffraction is defined as a superposition of two superimposed identical, within the region of their overlap, functions of the pupils of the speckle-fields for two exposures. Besides, when providing maximum values of the correlation functions, Eq. (5) for even phase function $\varphi(x_2, y_2)$, corresponding to the axial wave aberrations of a controllable lens, takes the following form:

$$\begin{aligned} u(x_4, y_4) \sim & \left\{ \exp(i\beta) \left\{ 1 + \exp i \left[\frac{\partial \varphi(\mu_2 x_4, \mu_2 y_4)}{\partial \mu_2 x_4} 2c \right] \right\} \times \right. \\ & \times \int_{-\infty}^{\infty} \int_{-\infty}^{\infty} t(\mu_1 \xi, \mu_1 \eta) \exp \left[\frac{-ik f_1 l_1 l_2}{(f_1 - l_1) L f_2^2} (x_4 \xi + y_4 \eta) \right] d\xi d\eta + \\ & + \exp(-i\beta) \left\{ 1 + \exp i \left[\frac{\partial \varphi(\mu_2 x_4, \mu_2 y_4)}{\partial \mu_2 x_4} 2c \right] \right\} \times \\ & \times \int_{-\infty}^{\infty} \int_{-\infty}^{\infty} t(-\mu_1 \xi, -\mu_1 \eta) \exp \left[\frac{ik f_1 l_1 l_2}{(f_1 - l_1) L f_2^2} (x_4 \xi + y_4 \eta) \right] d\xi d\eta \left. \right\} \otimes \\ & \otimes P_2(x_4, y_4), \end{aligned} \quad (6)$$

where $\frac{\xi f_1 l_1 l_2}{\lambda (f_1 - l_1) L f_2^2}$ and $\frac{\eta f_1 l_1 l_2}{\lambda (f_1 - l_1) L f_2^2}$ are the spatial frequencies, λ is the wavelength of the coherent light, used for the hologram recording and reconstruction, $\frac{\partial \varphi(\mu_2 x_4, \mu_2 y_4)}{\partial \mu_2 x_4} c = \varphi(\mu_2 x_4 + c, \mu_2 y_4) - \varphi(\mu_2 x_4, \mu_2 y_4)$.

Since the change of sign of variables in the second integral in Eq. (6) is compensated for by the change of limits of an integral, distribution of the complex field amplitude in the Fourier-plane the lens L_2 (see Fig. 1b) is defined by the following expression:

$$u(x_4, y_4) \sim \left\{ [\exp(i\beta) + \exp(-i\beta)] \times \right. \\ \left. \times \left\{ 1 + \exp i \left[\frac{\partial \varphi(\mu_2 x_4, \mu_2 y_4)}{\partial \mu_2 x_4} 2c \right] \right\} F_1(x_4, y_4) \right\} \otimes \\ \otimes P_2(x_4, y_4), \quad (7)$$

where

$$F_1(x_4, y_4) = \\ = \iint_{-\infty}^{\infty} t(\mu_1 \xi, \mu_1 \eta) \exp \left[\frac{-ik f_1 l_1 l_2}{(f_1 - l_1) L f_2^2} (x_4 \xi + y_4 \eta) \right] d\xi d\eta$$

is the Fourier transform of the corresponding function.

If the period of the function $[\exp(i\beta) + \exp(-i\beta)] \times \{1 + \exp i [\partial \varphi(\mu_2 x_4, \mu_2 y_4) / \partial \mu_2 x_4] 2c\}$ is at least one order longer than the size of a subjective speckle, this function can be factored out from the sign of the convolution integral (see Ref. 4). In this case, the illuminance distribution in the plane (x_4, y_4) takes the following form:

$$I(x_4, y_4) \sim \left\{ \left[1 + \cos \frac{\partial \varphi(\mu_2 x_4, \mu_2 y_4)}{\partial \mu_2 x_4} 2c \right] \times \right. \\ \left. \times \left[1 + \cos \frac{k f_1 l_1 l_2}{(f_1 - l_1) L f_2^2} (x_4^2 + y_4^2) \right] \right\} \times \\ \times \left| F_1(x_4, y_4) \otimes P_2(x_4, y_4) \right|^2. \quad (8)$$

Equation (8) describes the speckle-structure modulated by interference fringes, which represent the lateral shear interferogram in fringes of infinite width. The latter describe the axial wave aberrations of a lens under control L_1 (see Fig. 1a). Besides, this low-frequency interference pattern, in its turn, modulates, as known from Ref. 5, high-frequency one which represents a system of Young interference rings due to interference of the waves in (-1) and $(+1)$ diffraction orders. If the value of

$D = \sqrt{\lambda(f_1 - l_1)Lf_2^2/f_1 l_1 l_2}$ is much less than the period of the function $[\partial \varphi(\mu_2 x_4, \mu_2 y_4) / \partial \mu_2 x_4] 2c$, the illuminance distribution in the observation plane (see Fig. 1a) is described by the following expression:

$$I(x_4, y_4) \sim \left[1 + \cos \frac{\partial \varphi(\mu_2 x_4, \mu_2 y_4)}{\partial \mu_2 x_4} 2c \right] \times \\ \times \left| F_1(x_4, y_4) \otimes P_2(x_4, y_4) \right|^2. \quad (9)$$

As it follows from Eq. (9), the lateral shear interferogram, describing the axial wave aberrations of a lens L_1 , (see Fig. 1a) provides a two times higher sensitivity as compare to double-exposure hologram recording using the Leight-Upatnieks scheme (see Ref. 10). This is due to superposition of quasi-spherical waves, propagated in the same direction along the optical axis and diffracted in (-1) and $(+1)$ diffraction orders. Moreover, based on Eq. (5), two out of four waves added in the observation plane β (see Fig. 1b) are reversed with respect to other two waves and their wave fronts are rotated by 180° around the optical axis.

In addition to the general case of a Gabor hologram recording at $l_1 > 0$, let us consider special case when the lens L_1 is placed in the plane of the amplitude screen. If $l_1 = 0$, the previous analysis is valid and, as indicated in Fig. 1b, the lateral shear interferogram describing the axial wave aberrations of a lens with the double sensitivity at a fixed shear value is formed at the stage of the hologram reconstruction. Moreover, the same result is achieved when collimating system of positive lenses L_2 and L_3 transfers the image from the plane (x_3, y_3) into the plane (x_4, y_4) (see Fig. 2).

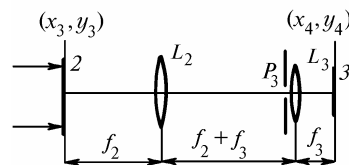


FIG. 2. Optical arrangement of recording of the interference pattern, localized in the hologram plane.

In the case of $l_1 = 0$ the field distribution in the photoplate plane (x_3, y_3) for two exposures (see Fig. 1a) can be expressed as an integral over independent parameters of plane waves, which are their amplitude, phase and direction of propagation (see Ref. 6). Then, in the region of dispersion of the spatial frequency corresponding to the Fresnel diffraction zone the hologram transmittance component due to diffuse scattering within the area of the exposure fields overlapping can be defined from the following expression:

$$\tau(x_3, y_3) \sim \{ \exp[ik(x_3^2 + y_3^2)/2l_2] \otimes \exp i\varphi(x_3, y_3) \} \times \\ \times \{ t(-x_3, -y_3) \exp -i\varphi(-x_3, -y_3) \otimes \exp[-ik(x_3^2 + y_3^2)/2l_2] \} +$$

$$\begin{aligned}
& + \{ \exp[-ik(x_3^2 + y_3^2)/2l_2] \exp -i\varphi(-x_3, -y_3) \} \times \\
& \times \{ t(x_3, y_3) \exp i\varphi(x_3, y_3) \otimes \exp[ik(x_3^2 + y_3^2)/2l_2] \} + \\
& + \{ \exp[ik(x_3^2 + y_3^2)/2l_2] \otimes \exp i\varphi(x_3 + a, y_3) \} \times \\
& \times \{ t(-x_3, -y_3) \exp -i\varphi(-x_3 + a, -y_3) \otimes \\
& \otimes \exp[-ik(x_3^2 + y_3^2)/2l_2] \} + \{ \exp[-ik(x_3^2 + y_3^2)/2l_2] \otimes \\
& \otimes \exp -i\varphi(-x_3 + a, -y_3) \} \{ t(x_3, y_3) \exp i\varphi(x_3 + a, y_3) \otimes \\
& \otimes \exp[ik(x_3^2 + y_3^2)/2l_2] \}. \quad (10)
\end{aligned}$$

If the spatial filtering of the diffraction field is made at the optical axis using objective aperture p_3 of the lens L_3 with the focal length f_3 (see Fig. 2) and in the case when the field is unlimited in space by the lens L_2 , one can show, using Ref. 7, that the complex field amplitude distribution in the observation plane takes the form

$$u(x_4, y_4) \sim \tau(-\mu_3 x_4, -\mu_3 y_4) \otimes P_3(x_4, y_4), \quad (11)$$

where $P_3(x_4, y_4)$ is the Fourier transform of the transmission function of the objective aperture of the lens L_3 (see Ref. 3); $\mu_3 = f_2/f_3$ is the coefficient of the scale transformation.

By substituting Eq. (10) into Eq. (11) and in view of the validity of equality

$$\begin{aligned}
& \{ \exp[ik(x_4^2 + y_4^2)\mu_3^2/2l_2] \otimes \exp i\varphi(-\mu_3 x_4, -\mu_3 y_4) \} \times \\
& \times \{ t(\mu_3 x_4, \mu_3 y_4) \exp -i\varphi(\mu_3 x_4, \mu_3 y_4) \otimes \\
& \otimes \exp[-ik(x_4^2 + y_4^2)\mu_3^2/2l_2] \} = \{ \exp[-ik(x_4^2 + y_4^2)\mu_3^2/2l_2] \times \\
& \times \exp -i\varphi(\mu_3 x_4, \mu_3 y_4) \} \{ t(-\mu_3 x_4, -\mu_3 y_4) \times \\
& \times \exp i\varphi(-\mu_3 x_4, -\mu_3 y_4) \otimes \exp[ik(x_4^2 + y_4^2)\mu_3^2/2l_2] \},
\end{aligned}$$

(which can be proved by writing the convolution in the integral form and assuming the even phase function, describing the axial wave aberrations of the lens, to be a slow changing function coordinates), one can obtain the following expression:

$$\begin{aligned}
u(x_4, y_4) \sim & \left\{ 1 + \exp i \left[\frac{\partial \varphi(\mu_3 x_4, \mu_3 y_4)}{\partial \mu_3 x_4} 2a \right] \right\} \times \\
& \times \left\{ t(\mu_3 x_4, \mu_3 y_4) \otimes \exp \left[-\frac{ik \mu_3^2}{2 l_2} (x_4^2 + y_4^2) \right] \right\} \otimes \\
& \otimes P_3(x_4, y_4). \quad (12)
\end{aligned}$$

Hence, on the basis of an earlier used condition implying, that if a subjective speckle defined by the width of the function $P_3(x_4, y_4)$ is small as compared to the speckle-field phase modulation period, the illuminance distribution in the plane (x_4, y_4) can be expressed in the following form:

$$I(x_4, y_4) \sim \left\{ 1 + \cos \left[\frac{\partial \varphi(\mu_3 x_4, \mu_3 y_4)}{\partial \mu_3 x_4} 2a \right] \right\} \times$$

$$\begin{aligned}
& \times \left| t(\mu_3 x_4, \mu_3 y_4) \otimes \exp \left[-\frac{ik \mu_3^2}{2 l_2} (x_4^2 + y_4^2) \right] \otimes \right. \\
& \left. \otimes P_3(x_4, y_4) \right|^2. \quad (13)
\end{aligned}$$

Equation (13) represents the lateral shear interferogram in the bands of infinite width, which modulates the subjective speckle-structure. Moreover, the interference pattern, localized in the hologram plane, describes the axial wave aberrations of the lens under control with doubled sensitivity at a fixed lateral shear.

In our experiments, the double-exposure holograms were recorded on the photoplates of Micrat VRS type using radiation of a He-Ne laser at $\lambda = 0.63 \mu\text{m}$. The experimental procedure includes a comparison of double-exposure holograms, recorded using Gabor and Leight-Upatnieks methods.

As an example, the lateral shear interferogram recorded at the stage of the hologram reconstruction in the course of spatial filtering of the diffraction field in the hologram plane at the optical axes in (-1) diffraction order using a small-aperture laser beam ($\approx 2 \text{ mm}$) (see Ref. 1) is shown in Fig. 3a. The interferogram localizes in the plane of imaginary image of a mat screen and describes spherical aberration with the afterfocal defocusing of the lens with focal length $f_1 = 120 \text{ mm}$ and pupil diameter $d_1 = 30 \text{ mm}$ under control. Double-exposure hologram recording was performed using an off-axis reference wave for $l_1 = 45 \text{ mm}$, $l_2 = 290 \text{ mm}$, $a = 0.2 \pm 0.002 \text{ mm}$, and $b = 0.32 \pm 0.002 \text{ mm}$. The lateral filtering of the diffraction field in the hologram plane out of the optical axis ($x_3 = 8 \text{ mm}$, $y_3 = 0$) causes the formation of the lateral shear interferogram (see Fig. 3b), which also describes the off-axis wave aberration of the lens under control (see Ref. 1).

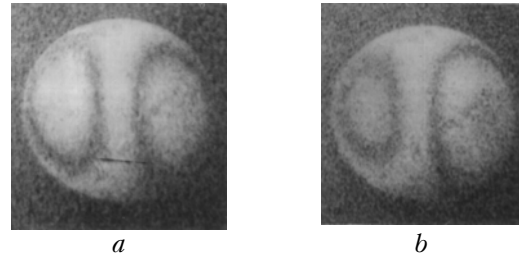


FIG. 3. Interference patterns, localized in the image plane of a mat screen and recorded with the spatial filtering of diffraction field in the hologram plane at the optical axis (a) and out of the optical axis (b).

Then, the amplitude diffuse screen was mounted instead of the mat screen, the channel forming the off-axis reference wave was eliminated and before the second exposure of the photoplate double-exposure recording of the hologram was performed with the Gabor method for $a = 0.2 \pm 0.002 \text{ mm}$, and $b = 0.32 \pm 0.002 \text{ mm}$. If, similarly to Ref. 1, the first and third terms in Eq. (3), determining the wave diffraction in $(+1)$ order are eliminated from the consideration, one can obtain the following. When

reconstructing the double-exposure Gabor hologram at the optical axis point using a small-aperture laser beam, the lateral shear interferogram, describing the wave aberrations of the lens, appears in the plane the imaginary image of the diffuse screen in (-1) diffraction order. But, if the spatial filtering is made in the region off of the optical axis, the interference pattern describes the off-axis wave aberration, as well. Thus, the results of the double-exposure Gabor hologram reconstruction at the point $x_3 = 8$ mm and $y_3 = 0$ using a small-aperture laser beam are shown in Fig. 4a. The unfocused twin of the imaginary image of the screen (real image) is in the right part of Fig. 4a, whereas a part of the interference pattern in the plane of the imaginary image of the diffuse screen, is the same as in Fig. 3b. When reconstructing the double-exposure Gabor hologram at the point of the optical axis, unfocused real image fully superimposes the imaginary diffuse screen image and luminosity of the interference pattern of the kind presented in Fig. 1a reduces to zero.

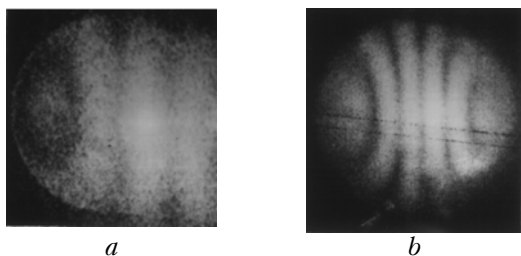


FIG. 4. Interference patterns, recorded in the course of double-exposure hologram reconstruction using spatial filtering of the diffraction field in the hologram plane in the region off of the optical axis (a) and at the optical axis in the near-diffraction zone (b).

As shown in Fig. 1b, when a double-exposure Gabor hologram is reconstructed using the spatial filtering at the optical axis in the Fourier plane in the near diffraction band, the lateral shear interferogram, presented in Fig. 4b, forms. This interferogram demonstrates doubled sensitivity of the interferometer to the lens axial wave aberrations. The interference pattern, recorded with the spatial filtering at the optical axis in the hologram plane (see Ref. 1) when the mat screen and photoplate shears before the second exposure were $a = 0.4 \pm 0.002$ mm and $b = 0.64 \pm 0.002$ mm, respectively, are presented in Fig. 5. Within the experimental errors, this pattern is identical to that presented in Fig. 4b.

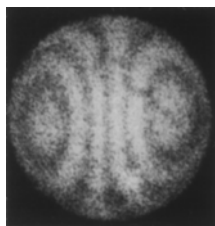


FIG. 5. Interference pattern, localized in the image plane of a mat screen.

Note that for the interference pattern shown in Fig. 4b to be recorded, the double-exposure Gabor hologram should be placed at the first focal plane of the lens L_2 (see Fig. 1b). Then, based on the phases of diverged and converged waves in the hologram plane (see Refs. 8, 9), the angular distribution of the waves in (-1) diffraction order scattered by the hologram fully overlaps in the Fourier plane with that in $(+1)$ diffraction order. Deviation from this hologram position causes partial overlap of the spectra within a lower solid angle which determines the decrease in spatial extension of the interference pattern. Besides, a displacement of the center of filtering aperture p_2 (see Fig. 1b) in the plane (x, y) leads to distortion of the interference pattern shown in Fig. 4b and affects its luminosity due to difference in propagation directions of the waves diffracted in (-1) and $(+1)$ orders of diffraction.

Similarly to Ref. 1, ignoring the first and third terms in Eq. (3), one can show, that for double-exposure Gabor hologram phase distortion of the reference wave (is seen in Fig. 1a, this distortion is determined by axial wave aberrations of the lens L_1) causes interference pattern to form in the hologram plane. For the pattern to be recorded spatial filtering of the diffraction field in (-1) diffraction order at the optical axis in the plane of the amplitude light diffuse screen image must be performed. However, luminosity of the interference pattern reduces to zero due to full superposition of the waves, diffracted in $(+1)$ order. If we consider, that displacement of the filtering aperture in the plane of the amplitude diffuse screen image (x, y) causes, as in Ref. 1, distortion of the interference pattern in the hologram plane and decreases its contrast due to off-axis wave aberrations of the lens under control, it is obvious, that the pattern can not be recorded even with partial spatial separation of the waves in (-1) and $(+1)$ diffraction orders, as it is made for spatial filtering of the diffraction field in the region off of the optical axis in the plane of the double-exposure Gabor lens hologram.

For double-exposure hologram recording with a lens, placed in the plane of the diffuse screen a plane-convex lens with the focal length $f_1 = 180$ mm and pupil diameter $d_1 = 30$ mm was used. The gap $z = 0.3$ mm between the lens and the screen satisfies the condition of "geometric shadow" $z \leq 0.2\rho^2/\lambda$ (see Ref. 10), where ρ is the radius of correlation between the diffuse screen inhomogeneities. The photoplate was placed at the distance $l_2 = 370$ mm.

Figure 6a shows the lateral shear interferogram, describing spherical aberration in paraxial focus of the lens under control. The interferogram was recorded with the spatial filtering of the diffraction field at the optical axis in the plane of the hologram whose double-exposure recording was made using an off-axis reference wave (see Ref. 1) at lateral shear $a = 1.5 \pm 0.002$ mm before second exposure. When performing the spatial filtering at the optical axis in the double-exposure Gabor hologram plane, the

distribution of the complex field amplitude in far diffraction zone for this hologram takes the following form:

$$\begin{aligned}
 u(x_4, y_4) \sim & \left\{ \left\{ 1 + \exp i \left[\frac{\partial \varphi(\mu_2 x_4, \mu_2 y_4)}{\partial \mu_2 x_4} a \right] \right\} \times \right. \\
 & \times \left\{ t(\mu_2 x_4, \mu_2 y_4) \exp -i \left[\varphi(\mu_2 x_4, \mu_2 y_4) + \frac{k(x_4^2 + y_4^2)}{2 l_2} \right] + \right. \\
 & \left. \left. + t(-\mu_2 x_4, -\mu_2 y_4) \exp i \left[\varphi(\mu_2 x_4, \mu_2 y_4) + \frac{k(x_4^2 + y_4^2)}{2 l_2} \right] \right\} \right\} \otimes \\
 & \otimes P_2(x_4, y_4) . \tag{14}
 \end{aligned}$$

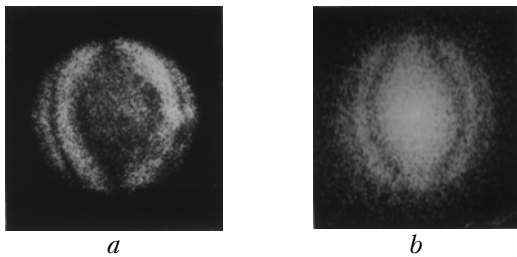


FIG. 6. Lateral shear interferograms, recorded with spatial filtering of the diffraction field at the optical axis in the plane of double-exposure hologram according to Leight-Upatnieks (a) and Gabor (b) schemes.

Superposition of the correlating speckle-fields for two exposures, in (−1) and (+1) diffraction orders, determines the illuminance distribution in the observation plane as

$$\begin{aligned}
 I(x_4, y_4) \sim & \left\{ 1 + \cos \left[\frac{\partial \varphi(\mu_2 x_4, \mu_2 y_4)}{\partial \mu_2 x_4} a \right] \right\} \times \\
 & \times \left\{ 1 \pm \cos \left[2\varphi(\mu_2 x_4, \mu_2 y_4) + \frac{k(x_4^2 + y_4^2)}{2 l_2} \right] \right\} \times \\
 & \times \left| t(\mu_2 x_4, \mu_2 y_4) \otimes P_2(x_4, y_4) \right|^2 , \tag{15}
 \end{aligned}$$

where the sign in second term depends on whether or not the function $t(x_1, y_1)$ is even.

Since the period of the function $2\varphi(\mu_2 x_4, \mu_2 y_4) + \frac{k(x_4^2 + y_4^2)}{2 l_2}$ is much shorter than that of the function $a [\partial \varphi(\mu_2 x_4, \mu_2 y_4) / \partial \mu_2 x_4]$, the lateral shear interferogram, describes, as shown in Fig. 6b, the axial aberrations of the lens, appears in the observation plane in the bands of infinite width.

But, according to Fig. 1b, reconstruction of the double-exposure hologram results in formation of the interference pattern, presented in Fig. 7a, while, as illustrated in Fig. 2, when reconstructing interference pattern, as shown in Fig. 7b, appears in the hologram

plane. As in the previous case, this pattern describes the axial wave aberrations of the lens under control with doubled sensitivity at a fixed lateral shear $a = 1.5 \pm 0.002$ mm. At the same time the luminosity of the interference pattern, presented in Fig. 7a, decrease with the lateral shear and it is universally lower than that of the pattern appeared in the hologram plane. This is due to diffraction of the background radiation from the corresponding non-overlapped areas of the lens pupil for two exposures. As shown in Fig. 1b, this radiation appears at the stage of the Gabor hologram reconstruction.

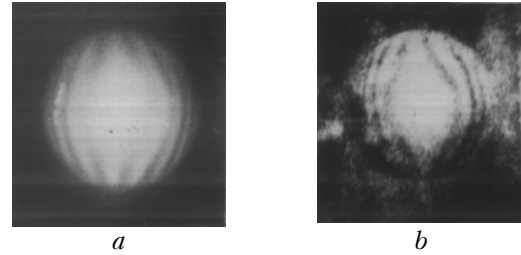


FIG. 7. Lateral shear interferogram in the far diffraction zone (a) and in the plane of a double-exposure Gabor hologram (b).

Thus, our experimental results indicate, that in the case of a double-exposure recording of the amplitude diffuse screen imaginary image using the Gabor scheme with a positive lens, correlation of the speckle-fields in (−1) and (+1) diffraction orders in the Fourier plane provides for the formation of the lateral shear interferogram in the bands of infinite width. That interferogram describes with a doubled sensitivity at a fixed shear wave aberrations of the lens. Besides, if the lens is placed in the diffuser plane, the double-exposure hologram recording provides for the localization of the interference pattern with double sensitivity, as well. This well agrees with Ref. 1, where it is shown, that the double-exposure recording of a mat screen imaginary image hologram using the off-axis reference wave causes the formation of the interference pattern in diffusely scattered fields, localized in the hologram plane and describes aberration of the reference wave. Hence, the physical reason for increase in the sensitivity of the lateral shear holographic interferometer presented is in the double passage of the reference and objective waves through the lens or objective under control, interference of waves in (−1) and (+1) diffraction orders and in the symmetry of the phase function, which describes the aberrations of the lens under control.

REFERENCES

1. V.G. Gusev, Atmos. Oceanic Opt. 5, No. 4, 219–225 (1992).
2. D. Goodman, Introduction to Fourier Optics (Mc Graw Hill, New York, 1968).
3. V.G. Gusev, Opt. Spektrosk. 69, 1125–1128 (1990).

4. R. Jones and C. Wykes, *Holographic and Speckle Interferometry* (Cambridge University Press, 1986).
5. M. Franson, *Optics of Specks* [Russian translation] (Mir, Moscow, 1980), 158 pp.
6. S.M. Rytov, *Introduction into the Statistical Radiophysics* (Nauka, Moscow, 1966), 404 pp.
7. V.G. Gusev, *Opt. Spektrosk.* **74**, No. 5, 989–994 (1993).
8. V.G. Gusev, *ibid.* **71**, No. 1, 171–174 (1991).
9. V.G. Gusev, *Lateral shear interferogram formation in diffusely scattered field under double-exposure Fourier hologram recording* (Dep. in VINITI, Moscow, Dec. 11, 1991, No. 4892–B91) 20 pp.
10. G.I. Vasilenko and L.M. Tsuibulkin, *Holographic recognition devices* (Radio i Svyaz', Moscow, 1985), 310 pp.